

Amplifying Frequency Up-Converted Infrared Signals with a Molecular Optomechanical Cavity

Fen Zou,^{1,2} Lei Du,³ Yong Li,^{1,*} and Hui Dong^{4,†}

¹Center for Theoretical Physics & School of Physics and Optoelectronic Engineering, Hainan University, Haikou 570228, China

²Beijing Computational Science Research Center, Beijing 100193, China

³Center for Quantum Sciences and School of Physics,

Northeast Normal University, Changchun 130024, China

⁴Graduate School of China Academy of Engineering Physics, Beijing 100193, China

(Dated: April 17, 2024)

Frequency up-conversion, enabled by molecular optomechanical coupling, has recently emerged as a promising approach for converting infrared signals into the visible range through quantum coherent conversion of signals. However, detecting these converted signals poses a significant challenge due to their inherently weak signal intensity. In this work, we propose an amplification mechanism capable of enhancing the signal intensity by a factor of 1000 or more for the frequency up-converted infrared signal in a molecular optomechanical system. The mechanism takes advantage of the strong coupling enhancement with molecular collective mode and Stokes sideband pump. This work demonstrates a feasible approach for up-converting infrared signals to the visible range.

Introduction—The mid- and far-infrared frequency range, encompassing wavelengths from 2.5 to 500 μm , is a critical region of the electromagnetic spectrum with significant applications in many fields, including thermal imaging [1], quantum sensing [2], microscopy [3, 4], clinical medicine [5], and astronomical surveys [6, 7]. However, detecting photons within this range presents a significant challenge, as conventional infrared detectors are sensitive to the thermal noise at the frequency vicinity of these photons, and require cryogenic temperatures to reduce this noise. As a result, there is a pressing need for improved detection technologies that can operate within this frequency range without the need for cryogenic cooling.

One promising approach is to utilize coherent up-conversion technology [8–14] to convert lower-frequency infrared (IR) light into the visible or near-infrared (VIS/NIR) range, which can be detected by using cost-effective and highly sensitive VIS/NIR cameras. This strategy takes advantage of the well-developed infrastructures and capabilities of VIS/NIR cameras, including their high integration and low cost, making it an attractive option for a wide range of applications. Recently, molecular optomechanical cavities have emerged as a promising candidate to achieve coherent frequency up-conversion [15]. In such systems, the molecular vibrational motion is bilinearly coupled to the IR field and optomechanically coupled to the VIS field to be converted into. The advantages of coupling multiple molecules and enhancing coupling strength via plasmonic nanocavities result in a significant enhancement of the detection efficiency [16, 17] beyond the conventional optomechanical cavity setups [18–31]. The question still remains as to whether this system is capable of detecting a weak IR signal at the few-photon level with enhanced sensitivity.

In this Letter, we propose a scheme to amplify the intensity for the frequency up-converted IR signal in the

molecular optomechanical system with a blue-detuned pump field, tuned close to the first Stokes sideband frequency of VIS mode. We show that the coherent IR signal of interest can be amplified by a factor of 1000 (or more). Such an amplification mechanism is proved to exist for the blue-detuned pump scheme, while being absent in the pioneer works with a red-detuned pump field [15–17]. Additionally we present the necessary stability analyses to show the parametric regions where the amplification scheme remains stable. The current theoretical study provides a routine strategy to analyze the up-converted IR detection, covering both amplification and stability considerations. And our amplification scheme will enable detecting the frequency up-converted IR signal of weak intensity.

Model.—The molecular optomechanical system consists of N molecules and a cavity supporting both VIS and IR modes, as shown in Fig. 1(a). The cavity modes may consist of plasmonic modes of nanoparticles [16, 17], supporting two plasmonic modes with frequencies ω_a in the VIS region (with annihilation operator a) and ω_c in the IR region (with annihilation operator c). Molecules are specifically chosen to couple with both the VIS and IR modes [15–17]. A strong pump field in the visible range with frequency ω_p and amplitude ε_p is applied to drive the VIS mode a in the cavity. The weak IR signal of interest with frequency ω_{ir} and amplitude ε_{ir} is incident on the cavity and couples to the IR mode c . In the interaction picture with respect to $H_0 = \hbar\omega_p a^\dagger a$, the

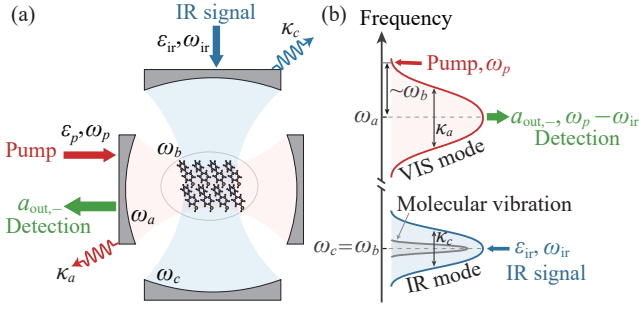


Figure 1. (a) The molecular optomechanical system consisting of N molecules (with frequency ω_b of the vibrational mode) coupled to both the VIS mode (with frequency ω_a and decay rate κ_a) via the optomechanical interaction and the IR mode (with frequency ω_c and decay rate κ_c) via the bilinear interaction. The VIS mode is driven by a pump field with frequency ω_p and amplitude ε_p . The IR signal of interest with frequency ω_{ir} and amplitude ε_{ir} is incident on the cavity with coupling to the IR mode c . (b) Scheme of frequency up-converted IR signals based on the molecular optomechanical system. Here the IR signal of interest is near-resonant with the vibrational frequency of the molecules (as well as the IR mode c) and the blue-detuned pump field is near-resonant with the first Stokes sideband of the VIS mode, i.e., $\omega_{ir} \simeq \omega_b = \omega_c$ and $\omega_p \simeq \omega_a + \omega_b$. The input weak IR signal with frequency ω_{ir} is up-converted as the output VIS signal ($a_{out,-}$) with frequency $\omega_p - \omega_{ir}$ via the optomechanical interaction between the VIS mode and the molecular vibration.

Hamiltonian of the system is given as ($\hbar = 1$)

$$\begin{aligned}
 H_{\text{sys}} = & \Delta_0 a^\dagger a + \omega_c c^\dagger c + \sum_{j=1}^N \omega_b b_j^\dagger b_j \\
 & + \sum_{j=1}^N g_a a^\dagger a (b_j^\dagger + b_j) + \sum_{j=1}^N g_c (c^\dagger + c) (b_j^\dagger + b_j) \\
 & + i(\varepsilon_p a^\dagger + \varepsilon_{ir} e^{-i\omega_{ir}t} c^\dagger - \text{H.c.}), \quad (1)
 \end{aligned}$$

where b_j (b_j^\dagger) is the annihilation (creation) operator of the vibrational mode of the j th molecule with frequency ω_b . The fourth term describes the optomechanical interaction between the VIS mode and the molecular vibration with the coupling strength g_a and the fifth term represents the bilinear interaction between the IR mode and the molecular vibration with the coupling strength g_c . The term including ε_p (ε_{ir}) describes the coupling of the pump field to the VIS mode (the coupling of the IR signal to the IR mode). The parameter $\Delta_0 = \omega_a - \omega_p$ is the detuning of the VIS mode with respect to the pump field. Without loss of generality, we assume these parameters (g_a , g_c , ε_p , and ε_{ir}) are real numbers.

By introducing the molecular collective operator $B = \sum_{j=1}^N b_j / \sqrt{N}$ satisfying $[B, B^\dagger] = 1$, the Hamiltonian in

Eq. (1) is simplified as

$$\begin{aligned}
 H = & \Delta_0 a^\dagger a + \omega_c c^\dagger c + \omega_b B^\dagger B + G_c (c^\dagger + c)(B^\dagger + B) \\
 & + G_a a^\dagger a (B^\dagger + B) + i(\varepsilon_p a^\dagger + \varepsilon_{ir} e^{-i\omega_{ir}t} c^\dagger - \text{H.c.}), \quad (2)
 \end{aligned}$$

where $G_a = g_a \sqrt{N}$ ($G_c = g_c \sqrt{N}$) is the collective optomechanical (bilinear) coupling strength. The corresponding quantum Langevin equations (QLEs) are obtained as

$$\dot{a} = -(i\Delta_0 + \kappa_a)a - iG_a a (B^\dagger + B) + \varepsilon_p + \sqrt{2\kappa_a} a_{in}, \quad (3a)$$

$$\dot{c} = -(i\omega_c + \kappa_c)c - iG_c (B^\dagger + B) + \varepsilon_{ir} e^{-i\omega_{ir}t} + \sqrt{2\kappa_c} c_{in}, \quad (3b)$$

$$\dot{B} = -(i\omega_b + \gamma_B)B - iG_a a^\dagger a - iG_c (c^\dagger + c) + \sqrt{2\gamma_B} B_{in}, \quad (3c)$$

where κ_a (κ_c) and γ_B are the decay rates of the VIS (IR) mode and the molecular collective mode respectively. a_{in} , c_{in} , and B_{in} are the noise operators with zero mean values $\langle o_{in} \rangle = 0$ for $o = a, c, B$. The amplitude of the IR signal ε_{ir} of interest is much smaller than that of the pump field ε_p , and is therefore treated as a perturbation. The relations between steady-state mean values of the operators are obtained by neglecting the term $\varepsilon_{ir} \exp(-i\omega_{ir}t)$ in Eq. (3b) as $\langle c \rangle_{ss} = -iG_c (\langle B \rangle_{ss} + \langle B \rangle_{ss}^*) / (i\omega_c + \kappa_c)$, $\langle B \rangle_{ss} = -i[G_a |\langle a \rangle_{ss}|^2 + G_c (\langle c \rangle_{ss} + \langle c \rangle_{ss}^*)] / (i\omega_b + \gamma_B)$, and $\langle a \rangle_{ss} = \varepsilon_p / (i\Delta + \kappa_a)$. Here $\Delta = \Delta_0 + G_a (\langle B \rangle_{ss} + \langle B \rangle_{ss}^*)$ represents the effective detuning, modified by the collective optomechanical interaction. These steady-state mean values are solved self-consistently.

The up-converted IR signal is analyzed via the quantum fluctuation $\delta o = o - \langle o \rangle_{ss}$ ($o = a, c, B$) on top of the steady-state value [32]. By keeping only the first-order term of quantum fluctuation, we obtain the linearized QLEs as

$$\begin{aligned}
 \delta \dot{a} = & -(i\Delta + \kappa_a)\delta a - i\mathcal{G}_a (\delta B^\dagger + \delta B) + \sqrt{2\kappa_a} a_{in}, \\
 \delta \dot{c} = & -(i\omega_c + \kappa_c)\delta c - iG_c (\delta B^\dagger + \delta B) + \varepsilon_{ir} e^{-i\omega_{ir}t} \\
 & + \sqrt{2\kappa_c} c_{in}, \\
 \delta \dot{B} = & -(i\omega_b + \gamma_B)\delta B - i(\mathcal{G}_a^* \delta a + \mathcal{G}_a \delta a^\dagger) \\
 & - iG_c (\delta c + \delta c^\dagger) + \sqrt{2\gamma_B} B_{in}, \quad (4)
 \end{aligned}$$

where $\mathcal{G}_a = G_a \langle a \rangle_{ss}$ is the enhanced collective optomechanical coupling strength due to the strong pump field. Note that the $\varepsilon_{ir} \exp(-i\omega_{ir}t)$ term is now included in Eq. (4). Here we do not employ the rotating-wave approximation for either the optomechanical or bilinear interaction terms.

To solve the linearized QLEs (4), we use the ansatz $\langle \delta o \rangle = o_+ e^{-i\omega_{ir}t} + o_- e^{i\omega_{ir}t}$ for $o = a, c, B$ [32–35], where o_+ and o_- correspond to the values of positive- and negative-frequency components. With this ansatz, o_\pm and o_\pm^* are solved analytically with their exact expressions presented in the Supplementary Material [36–38].

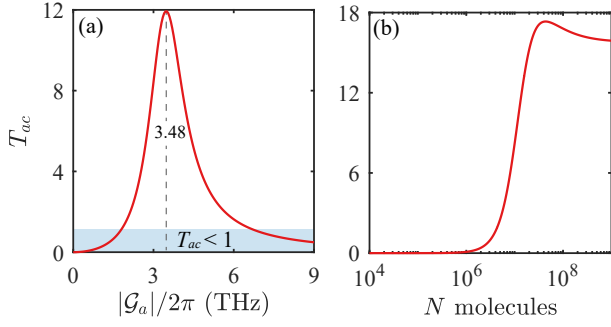


Figure 2. (a) The conversion efficiency T_{ac} as a function of the enhanced collective optomechanical coupling strength $|\mathcal{G}_a|$ for $N = 10^7$. (b) The conversion efficiency T_{ac} as a function of the number of the molecules N at $g_a/2\pi = 0.08$ GHz. Here we consider the resonance case $\omega_{ir} = \omega_b = \omega_c = 2\pi \times 30$ THz and other parameters are $\Delta = -\omega_b$, $\kappa_a/2\pi = 30$ THz, $\kappa_c/2\pi = 0.5$ THz, $\gamma_B/2\pi = 0.16$ THz, $\varepsilon_p/2\pi = 500$ THz, and $g_c/2\pi = 0.1$ GHz.

Amplification.—The IR signal of interest is amplified when the frequency of the blue-detuned pump field is tuned close to the first Stokes sideband of the VIS mode, i.e., $\Delta \simeq -\omega_b$. The up-converted signal is included in the quantum fluctuation δa of the VIS mode. The detection is performed on the output field of the VIS mode, denoted as $a_{out} = \langle a_{out} \rangle_{ss} + \delta a_{out}$, where $\langle a_{out} \rangle_{ss}$ (δa_{out}) is the steady-state (fluctuation) component of the output field a_{out} . The mean value of the fluctuation component is rewritten as $\langle \delta a_{out} \rangle = a_{out,+} e^{-i\omega_{ir}t} + a_{out,-} e^{i\omega_{ir}t}$, where $a_{out,+}$ and $a_{out,-}$ are the first anti-Stokes and Stokes components of $\langle \delta a_{out} \rangle$, respectively. With the input-output relation $a_{out} + a_{in} + \varepsilon_p/\sqrt{2\kappa_a} = \sqrt{2\kappa_a}a$ [39], we obtain the output signal as $a_{out,\pm} = \sqrt{2\kappa_a}a_{\pm}$.

In the case of the blue-detuned pump field with $\Delta = -\omega_b$, our main focus is on the upconversion at the first Stokes sideband. For the near-resonant case $\omega_{ir} \simeq \omega_b = \omega_c$, the first Stokes component a_- is obtained explicitly as [36]

$$a_- = \frac{2i\varepsilon_{ir}\mathcal{G}_a G_c \Delta (\Delta - \omega_{ir} + i\kappa_a) (\Delta - \omega_{ir} + i\kappa_c)}{\mathcal{A}(\omega_{ir})}, \quad (5)$$

where $\mathcal{A}(\omega_{ir}) = \{[\Delta^2 - (\omega_{ir} - i\kappa_c)^2][\Delta^2 - (\omega_{ir} - i\gamma_B)^2] - 4G_c^2\Delta^2\}[\Delta^2 - (\omega_{ir} - i\kappa_a)^2] + 4|\mathcal{G}_a|^2\Delta^2[\Delta^2 - (\omega_{ir} - i\kappa_c)^2]$. For the input IR signal $\varepsilon_{ir}/\sqrt{2\kappa_c}$ [36], the conversion efficiency T_{ac} at the first Stokes sideband is obtained as

$$T_{ac} = |t_{ac}|^2 = \left| \frac{2\sqrt{\kappa_a\kappa_c}a_-}{\varepsilon_{ir}} \right|^2, \quad (6)$$

where $t_{ac} \equiv a_{out,-}/(\varepsilon_{ir}/\sqrt{2\kappa_c})$ denotes the conversion coefficient from the IR signal to VIS range at the first Stokes sideband [35, 40].

For simplicity, we first consider the case where the IR signal is fully resonant with the vibrational frequency

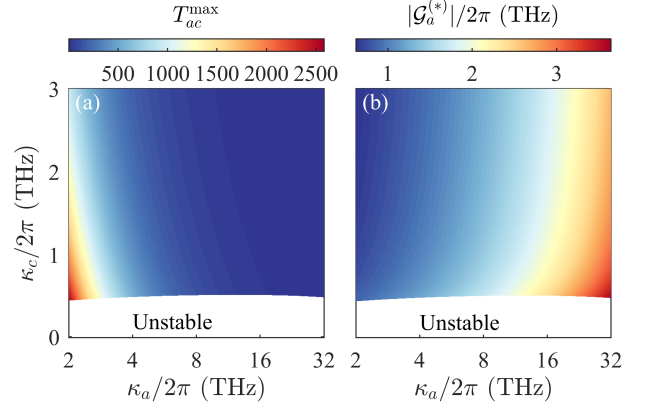


Figure 3. (a) The maximum conversion efficiency T_{ac}^{\max} as functions of the decay rates κ_a and κ_c at optimal coupling strength $|\mathcal{G}_a| = |\mathcal{G}_a^*| \simeq \sqrt{(G_c^2|\eta_c^{-1}| + \kappa_c\gamma_B|\eta_B|)\kappa_a|\eta_a|/\kappa_c}$. (b) The optimal coupling strength $|\mathcal{G}_a^*|$ as functions of the decay rates κ_a and κ_c . Here $N = 10^7$ and other parameters are the same as those in Fig. 2.

of the molecules (as well as the IR mode), i.e., $\omega_{ir} = \omega_b = \omega_c$. In this case, the conversion coefficient is $t_{ac} = 2\sqrt{\kappa_a\kappa_c}\mathcal{G}_a G_c / (G_c^2\kappa_a\eta_c^{-1} - |\mathcal{G}_a|^2\kappa_c\eta_a^{-1} + \kappa_a\kappa_c\gamma_B\eta_B)$, where $\eta_{a,c} = 1 + i\kappa_{a,c}/(2\Delta)$ and $\eta_B = 1 + i\gamma_B/(2\Delta)$ [36].

Figure 2(a) shows the conversion efficiency T_{ac} as a function of the enhanced collective optomechanical coupling strength $|\mathcal{G}_a|$ at the first Stokes sideband $\Delta = -\omega_b$. In our numerical simulations, we choose the experimentally feasible parameters [16, 17, 41–49] as $\omega_{ir}/2\pi = \omega_b/2\pi = \omega_c/2\pi = 30$ THz, $\kappa_a/2\pi = 30$ THz, $\kappa_c/2\pi = 0.5$ THz, $\gamma_B/2\pi = 0.16$ THz, $\varepsilon_p/2\pi = 500$ THz, $g_c/2\pi = 0.1$ GHz, and $N = 10^7$. One scheme for realizing the molecular optomechanical system involves an Au nanoparticle inside a nanogroove etched in a gold film to form the plasmonic cavity. Biphenyl-4-thiol molecules are chosen to support a prominent vibrational mode that couples to both the VIS and IR modes in the plasmonic cavity [16]. The single-photon optomechanical coupling strength between the VIS mode and the molecular vibration can reach $g_a \sim 2\pi \times 100$ GHz [44]. For other molecules, such as rhodamine 6G molecule, the single-photon optomechanical coupling strength g_a is within the range $2\pi \times (0.006 - 145)$ MHz [45]. Theoretically, the number of the molecules N in the cavity and the optomechanical coupling strength g_a are affected by the size of plasmonic cavity. Increasing the cavity size leads to a higher number of molecules but a decreased coupling strength [15, 44]. However, the overall effect of amplification is determined by the enhanced collective coupling strength \mathcal{G}_a , which can be further enhanced with the average photon number $\langle a \rangle_{ss}$. Detailed discussions on the impact of the number of the molecules and the coupling strength are presented in the Supplementary Material [36].

The curve in Fig. 2(a) shows that T_{ac} exceeds unity under the appropriate coupling strength condition to achieve the amplification of frequency up-converted IR signal. Moreover, the conversion efficiency of the IR signal reaches a maximum (i.e., $T_{ac}^{\max} \approx 12$) at optimal coupling strength [36] $|\mathcal{G}_a| = |\mathcal{G}_a^{(*)}| \simeq \sqrt{(G_c^2 |\eta_c^{-1}| + \kappa_c \gamma_B |\eta_B|) \kappa_a |\eta_a| / \kappa_c} = 2\pi \times 3.48$ THz for the given parameters. This trend inversion of the conversion efficiency occurs due to the requirement of matching relationship between two transfer processes described by the beam-splitting interaction ($G_c \delta B^\dagger \delta c + h.c.$) and the two-mode-squeezing one ($\mathcal{G}_a \delta a^\dagger \delta B^\dagger + h.c.$). The incoming IR signal is firstly converted into the molecular collective mode δB , which is then amplified into the VIS mode δa^\dagger . For the case with $\omega_b = \omega_c = -\Delta$, the two-mode-squeezing coupling Hamiltonian ($\mathcal{G}_a \delta a^\dagger \delta B^\dagger + h.c.$) can be diagonalized in terms of two new normal (Bogoliubov) modes, whose eigenvalues deviate largely from ω_b when the coupling strength is too strong. In this too-strong coupling case, the beam-splitting coupling ($G_c \delta B^\dagger \delta c + h.c.$) can be seen as the largely-detuned coupling between the IR mode and the two normal modes. Hence, once the coupling strength $|\mathcal{G}_a|$ is too strong (the two transfer processes are far away from the matching requirement), the IR signal cannot be converted to the molecular collective mode and the VIS mode. In Fig. 2(b), we illustrate the dependence of the conversion efficiency T_{ac} of the IR signal on the number of molecules. The curve shows a non-monotonic behavior with the highest conversion efficiency occurring at $N \sim 10^7$. Additionally, the curve shows a plateau where the conversion efficiency stays constant when the number of molecules is sufficiently large.

Other key parameters that determine the conversion efficiency of the IR signal are the decay rates κ_c and κ_a of the IR and VIS modes. In Fig. 3(a), we plot the maximum conversion efficiency T_{ac}^{\max} at the first Stokes sideband as functions of the decay rates κ_a and κ_c at optimal coupling strength $|\mathcal{G}_a^{(*)}|$. For a fixed decay rate κ_c (e.g. $\kappa_c/2\pi = 1$ THz), T_{ac}^{\max} is significantly improved by decreasing the decay rate κ_a of the cavity VIS mode. However, when the decay rate κ_a is fixed (e.g. $\kappa_a/2\pi = 30$ THz), T_{ac}^{\max} increases slowly with the increase of the decay rate κ_c of the cavity IR mode. In particular, the conversion efficiency T_{ac} with a factor around 1000 is achieved at $\kappa_a/2\pi = 2$ THz (i.e., $\kappa_a/\omega_b = 1/15$). These results highlight the importance of controlling the decay rates of the IR and VIS modes for amplifying frequency up-converted IR signal. Figure 3(b) shows the optimal coupling strength $|\mathcal{G}_a^{(*)}|$ as functions of the decay rates κ_a and κ_c . The results show that the optimal coupling strength $|\mathcal{G}_a^{(*)}|$ increases (decreases) as the value of κ_a (κ_c) increases.

The molecular optomechanical system could become unstable once the optomechanical and bilinear coupling

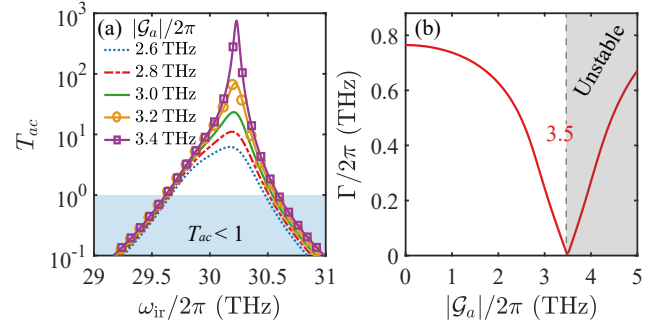


Figure 4. (a) The conversion efficiency T_{ac} as a function of the frequency of the IR signal ω_{ir} for different values of $|\mathcal{G}_a|$. (b) The bandwidth Γ as a function of the enhanced collective optomechanical coupling strength $|\mathcal{G}_a|$. Here $N = 10^7$ and other parameters are the same as those in Fig. 2. In panel (b), the unstable region is marked with the grey shadow.

strengths are strong enough [50]. We check the stability of the system with amplification and mark the unstable region in Fig. 3. The stability condition of the system is given explicitly according to the Routh-Hurwitz criterion [51, 52]. Mathematically, the system is stable only if the real parts of all the eigenvalues of the coefficient matrix [see Eq. (S10) in the Supplementary Material] are positive. Physically, the negative real part of the eigenvalue of this coefficient matrix represents the gain for the related diagonalized normal mode causing the instability. The detailed discussion of the stability is presented in the Supplementary Material [36].

Bandwidth of the amplification.—Another key characteristic of the up-conversion is the bandwidth of the detection. In the following, we explore the dependence of the conversion efficiency on the frequency of the IR signal of interest. For the near-resonant incident IR signal with $\omega_{ir} \simeq \omega_b = \omega_c$, the conversion efficiency of the IR signal to the VIS range at the first Stokes sideband is obtained as $T_{ac} = |4\sqrt{\kappa_a \kappa_c} \mathcal{G}_a G_c \Delta (\Delta - \omega_{ir} + i\kappa_a) (\Delta - \omega_{ir} + i\kappa_c) / \mathcal{A}(\omega_{ir})|^2$. Figure 4(a) shows the conversion efficiency T_{ac} as a function of the frequency ω_{ir} of the IR signal for different enhanced collective optomechanical coupling strengths \mathcal{G}_a . As $|\mathcal{G}_a|$ increases, the maximum conversion efficiency of the IR signal as well as the range of the amplification increases. For the resonant case $\omega_{ir} = \omega_b = \omega_c$, the maximum conversion efficiency ($T_{ac}^{\max} \approx 12$) is obtained at $|\mathcal{G}_a|/2\pi \approx 3.48$ THz, as shown in Fig. 2(a). However, for the near-resonant incident IR signal with $\omega_{ir} \simeq \omega_b = \omega_c$, we find higher amplification than that the resonance case for the frequency up-conversion. For example, the maximum conversion efficiency T_{ac}^{\max} of the IR signal is approximately 750 at $|\mathcal{G}_a|/2\pi = 3.4$ THz, and the range of the amplification for IR signal is 29.6 THz $\lesssim \omega_{ir}/2\pi \lesssim 30.6$ THz.

The bandwidth Γ of the conversion efficiency is obtained by estimating the full width at half maximum [50, 53]. In Fig. 4(b), we illustrate the bandwidth Γ as a func-

tion of the enhanced collective optomechanical coupling strength $|\mathcal{G}_a|$, with the unstable region marked with the gray shadow. The bandwidth Γ decreases with the increase of $|\mathcal{G}_a|$ in the stable region. At $|\mathcal{G}_a|/2\pi \approx 3.5$ THz, we observe that the bandwidth is $\Gamma \approx 0$ for the near-resonant case $\omega_{\text{ir}} \simeq \omega_b = \omega_c$, where the conversion efficiency of the IR signal diverges. The current figure illustrates a trade-off between the conversion efficiency and the bandwidth for choosing the proper coupling strength $|\mathcal{G}_a|$. The bandwidth of the conversion efficiency is determined by the optomechanical coupling strength g_a , the bilinear coupling strength g_c , and the decay rate of the molecular vibration γ_B . Detailed discussions about their effects on the bandwidth are presented in the Supplementary Material [36]. To increase the bandwidth Γ , one can use molecules with large decay rate of vibration γ_B . We also present the equivalent analyses of the conversion efficiency and the bandwidth with the power spectrum method [53, 54] in the Supplementary Material [36] to confirm the current results.

Conclusion and remarks.—We have proposed an amplification scheme to increase the sensitivity of detecting coherent IR signal in the molecular optomechanical systems, where the IR signal is up-converted into the visible range. In our scheme, the IR signal of interest is resonant (or near-resonant) with the molecular vibration, and the blue-detuned pump field, which is near-resonant with the first Stokes sideband of the VIS mode, is utilized to pump the cavity mode. We demonstrate the amplification by a factor of several thousands at the first Stokes sideband of the VIS mode with designed parameters of the cavity and the molecules and verify the existence of the stability of scheme. It is worth noting that such an amplification mechanism is absent for the case of the red-detuned pump field. Detailed discussions on the conversion efficiency for a red-detuned pump field are presented in the Supplementary Material. Furthermore, we show the new aspect with stability analysis, which is important for signal detection in both blue- and red-detuned regions (see the Supplementary Material). Our scheme shall provide insight into designing efficient up-conversion detection of IR signal on the few-photon level.

This work is supported by the National Natural Science Foundation of China (Grants No. 12088101, No. 12074030, No. 12274107, and No. U2230402) and the China Postdoctoral Science Foundation (Grant No. 2021M700360).

* yongli@hainanu.edu.cn

† hdong@gscaep.ac.cn

- [1] M. Tonouchi, *Nat. Photonics* **1**, 97 (2007).
 [2] M. Kutas, B. Haase, P. Bickert, F. Rixinger, D. Molter, and G. von Freymann, *Sci. Adv.* **6**, eaaz8065 (2020).
 [3] I. Kviatkovsky, H. M. Chrzanowski, E. G. Avery, H. Bar-

- tolomaeus, and S. Ramelow, *Sci. Adv.* **6**, eabd0264 (2020).
 [4] A. V. Paterova, S. M. Maniam, H. Yang, G. Grecni, and L. A. Krivitsky, *Sci. Adv.* **6**, eabd0460 (2020).
 [5] S. De Bruyne, M. M. Speeckaert, and J. R. Delanghe, *Crit. Rev. Clin. Lab. Sci.* **55**, 1 (2018).
 [6] S. Ariyoshi, K. Nakajima, A. Saito, T. Taino, C. Otani, H. Yamada, S. Ohshima, J. Bae, and S. Tanaka, *Supercond. Sci. Technol.* **29**, 035012 (2016).
 [7] T. L. Roellig, C. W. McMurtry, T. P. Greene, T. Matsuo, I. Sakon, and J. G. Staguhn, *J. Astron. Telesc. Instrum. Syst.* **6**, 041503 (2020).
 [8] E. J. Heilweil, *Opt. Lett.* **14**, 551 (1989).
 [9] T. P. Dougherty and E. J. Heilweil, *Opt. Lett.* **19**, 129 (1994).
 [10] K. Karstad, A. Stefanov, M. Wegmuller, H. Zbinden, N. Gisin, T. Aellen, M. Beck, and J. Faist, *Opt. Lasers Eng.* **43**, 537 (2005).
 [11] G. Temporão, S. Tanzilli, H. Zbinden, N. Gisin, T. Aellen, M. Giovannini, and J. Faist, *Opt. Lett.* **31**, 1094 (2006).
 [12] P. Tidemand-Lichtenberg, J. S. Dam, H. V. Andersen, L. Høgstedt, and C. Pedersen, *J. Opt. Soc. Am. B* **33**, D28 (2016).
 [13] Y.-P. Tseng, C. Pedersen, and P. Tidemand-Lichtenberg, *Opt. Mater. Express* **8**, 1313 (2018).
 [14] A. Barh, P. J. Rodrigo, L. Meng, C. Pedersen, and P. Tidemand-Lichtenberg, *Adv. Opt. Photon.* **11**, 952 (2019).
 [15] P. Roelli, D. Martin-Cano, T. J. Kippenberg, and C. Galland, *Phys. Rev. X* **10**, 031057 (2020).
 [16] W. Chen, P. Roelli, H. Hu, S. Verlekar, S. P. Amirtharaj, A. I. Barreda, T. J. Kippenberg, M. Kovylyna, E. Verhagen, A. Martínez, and C. Galland, *Science* **374**, 1264 (2021).
 [17] A. Xomalis, X. Zheng, R. Chikkaraddy, Z. Koczor-Benda, E. Miele, E. Rosta, G. A. E. Vandenbosch, A. Martínez, and J. J. Baumberg, *Science* **374**, 1268 (2021).
 [18] L. Tian and H. Wang, *Phys. Rev. A* **82**, 053806 (2010).
 [19] C. Dong, V. Fiore, M. C. Kuzyk, and H. Wang, *Science* **338**, 1609 (2012).
 [20] J. T. Hill, A. H. Safavi-Naeini, J. Chan, and O. Painter, *Nat. Commun.* **3**, 1196 (2012).
 [21] F. Ruesink, J. P. Mathew, M.-A. Miri, A. Alù, and E. Verhagen, *Nat. Commun.* **9**, 1798 (2018).
 [22] T. A. Palomaki, J. W. Harlow, J. D. Teufel, R. W. Simmonds, and K. W. Lehnert, *Nature (London)* **495**, 210 (2013).
 [23] Y.-D. Wang and A. A. Clerk, *Phys. Rev. Lett.* **108**, 153603 (2012).
 [24] L. Tian, *Phys. Rev. Lett.* **108**, 153604 (2012).
 [25] J. Bochmann, A. Vainsencher, D. D. Awschalom, and A. N. Cleland, *Nat. Phys.* **9**, 712 (2013).
 [26] R. W. Andrews, R. W. Peterson, T. P. Purdy, K. Cicak, R. W. Simmonds, C. A. Regal, and K. W. Lehnert, *Nat. Phys.* **10**, 321 (2014).
 [27] M. Forsch, R. Stockill, A. Wallucks, I. Marinković, C. Gärtner, R. A. Norte, F. van Otten, A. Fiore, K. Srinivasan, and S. Gröblacher, *Nat. Phys.* **16**, 69 (2020).
 [28] A. Metelmann and A. A. Clerk, *Phys. Rev. Lett.* **112**, 133904 (2014).
 [29] A. Nunnenkamp, V. Sudhir, A. K. Feofanov, A. Roulet, and T. J. Kippenberg, *Phys. Rev. Lett.* **113**, 023604 (2014).

- [30] A. Metelmann and A. A. Clerk, *Phys. Rev. X* **5**, 021025 (2015).
- [31] Z. Shen, Y.-L. Zhang, Y. Chen, F.-W. Sun, X.-B. Zou, G.-C. Guo, C.-L. Zou, and C.-H. Dong, *Nat. Commun.* **9**, 1797 (2018).
- [32] S. Weis, R. Rivière, S. Deléglise, E. Gavartin, O. Arcizet, A. Schliesser, and T. J. Kippenberg, *Science* **330**, 1520 (2010).
- [33] G. S. Agarwal and S. Huang, *Phys. Rev. A* **81**, 041803(R) (2010).
- [34] X.-W. Xu and Y. Li, *Phys. Rev. A* **92**, 023855 (2015).
- [35] H. Zhang, F. Saif, Y. Jiao, and H. Jing, *Opt. Express* **26**, 25199 (2018).
- [36] See Supplementary Material at [url] for detailed derivations, which includes Refs. [37,38].
- [37] X.-W. Xu and Y. Li, *Phys. Rev. A* **91**, 053854 (2015).
- [38] G. S. Agarwal and S. Huang, *Phys. Rev. A* **85**, 021801 (2012).
- [39] C. W. Gardiner and M. J. Collett, *Phys. Rev. A* **31**, 3761 (1985).
- [40] Y. Li, Y. Y. Huang, X. Z. Zhang, and L. Tian, *Opt. Express* **25**, 18907 (2017).
- [41] A. Shalabney, J. George, J. Hutchison, G. Pupillo, C. Genet, and T. W. Ebbesen, *Nat. Commun.* **6**, 5981 (2015).
- [42] J. P. Long and B. S. Simpkins, *ACS Photonics* **2**, 130 (2015).
- [43] F. Benz, M. K. Schmidt, A. Dreismann, R. Chikkaraddy, Y. Zhang, A. Demetriadou, C. Carnegie, H. Ohadi, B. de Nijs, R. Esteban, J. Aizpurua, and J. J. Baumberg, *Science* **354**, 726 (2016).
- [44] P. Roelli, C. Galland, N. Piro, and T. J. Kippenberg, *Nat. Nanotechnol.* **11**, 164 (2016).
- [45] M. K. Schmidt, R. Esteban, A. González-Tudela, G. Giedke, and J. Aizpurua, *ACS Nano* **10**, 6291 (2016), and also in Supplementary materials.
- [46] A. Lombardi, M. K. Schmidt, L. Weller, W. M. Deacon, F. Benz, B. de Nijs, J. Aizpurua, and J. J. Baumberg, *Phys. Rev. X* **8**, 011016 (2018).
- [47] S. Pannir-Sivajothi, J. A. Campos-Gonzalez-Angulo, L. A. Martínez-Martínez, S. Sinha, and J. Yuen-Zhou, *Nat. Commun.* **13**, 1645 (2022).
- [48] R. Esteban, J. J. Baumberg, and J. Aizpurua, *Acc. Chem. Res.* **55**, 1889 (2022).
- [49] R. Chikkaraddy, A. Xomalis, L. A. Jakob, and J. J. Baumberg, *Light Sci. Appl.* **11**, 19 (2022).
- [50] C. Jiang, L. N. Song, and Y. Li, *Phys. Rev. A* **97**, 053812 (2018).
- [51] E. X. DeJesus and C. Kaufman, *Phys. Rev. A* **35**, 5288 (1987).
- [52] I. S. Gradshteyn and I. M. Ryzhik, *Table of integrals, series, and products* (Academic press, 2014).
- [53] D. Malz, L. D. Tóth, N. R. Bernier, A. K. Feofanov, T. J. Kippenberg, and A. Nunnenkamp, *Phys. Rev. Lett.* **120**, 023601 (2018).
- [54] A. A. Clerk, M. H. Devoret, S. M. Girvin, F. Marquardt, and R. J. Schoelkopf, *Rev. Mod. Phys.* **82**, 1155 (2010).